

## IMPROVED TIMING RECOVERY IN WIRELESS MOBILE RECEIVERS

T. O. Olwal, M. A. van Wyk, B. J. van Wyk, M. Odhiambo, and D. Chatelain

French South Africa Technical Institute of Electronics. Private Bag X680, Pretoria, 0001,  
Republic of South Africa. Tshwane University of Technology  
Email: thomasolwal@yahoo.ca

**ABSTRACT:-** *The problem of timing recovery in wireless mobile receiver systems is critical. This is partly because timing recovery functions must follow rapid parameter changes inherent in mobile systems and partly because both bandwidth and power must be conserved in low signal to noise ratio communication channels. The ultimate goal is therefore to achieve a low bit error rate on the recovered information for improving QoS provisioning to terminal mobile users. Traditional timing recovery methods have over-relied on phase-locked loops for timing information adjustment. However, associated schemes do not exploit code properties. This leads to synchronization difficulties in digital receivers separated from transmitters by lossy channels. In this paper we present a soft timing phase estimation algorithm for wireless mobile receivers in low signal to noise ratios. In order to develop a bandwidth and power efficient timing recovery method for wireless mobile receivers, a raised cosine filter and a multilevel phase shift keying modulation scheme are implemented and no clock signals are transmitted to the receiver. In the proposed method, the receiver exploits the soft decisions computed at each turbo decoding iteration to provide reliable estimates of a soft timing signal, which in turn, improves the decoding time. The derived method, based on sequential minimization techniques, approaches the theoretical Cramer-Rao bound with unbiased estimates within a few iterations.*

**Key Words:** *discrete polyphase matched filters, maximum likelihood estimators, iterative turbo receivers, log-MAP based soft signals, Sequential unconstrained extremization techniques, SOVA based soft signals.*

### 1. INTRODUCTION

In the recent past, most wireless mobile communication systems have over-relied on classical forward error correction (FEC) codes to either save bandwidth or reduce power requirements [1]. However, classical FEC coding schemes have limited coding gain. Wireless cellular mobile receivers in a number of recent publications employ data-aided (DA) synchronizers based on the Viterbi algorithm for optimum signal detection to achieve accuracy, reliability and fast speed convergence [2]. However, DA timing phase recovery is bandwidth and power inefficient since additional bandwidth and power is needed to transmit clock signals to the receiver from the transmitter.

For quality of service (QoS) provisioning, the bandwidth and power conservation, the speed of convergence and a jitter free timing synchronization is desirable. In low signal to noise ratio environments, achieving good bandwidth and power transmission efficiencies as well as a jitter free timing phase estimation is a challenging task [3]. This is partly because of spectrally inefficient modulation schemes and transmission filters which are currently being employed in most 2<sup>nd</sup> generation wireless cellular mobile systems [4] and partly because of computational complexities related to the system mobility and timing recovery in low SNR scenarios. Fortunately, the impressive performance of turbo codes has triggered the application of this powerful

coding technique to digital communications in low SNR environments [5]-[7]. Several receiver functions such as the signal detection, equalization, demodulation and timing recovery, are now possible with a combined turbo decoding algorithm [8]-[10].

Most classical timing phase estimation schemes are separated from the decoding process with little penalty: This is in the sense that a timing recovery uses an instantaneous decision device to provide tentative decisions that are adequately reliable. The reliable decisions are used to estimate the timing phase error [11]. Classical timing recovery methods also assume that the neighbouring symbols are mutually independent at high SNR and the associated theoretical framework is normally based on least mean square (LMS) and traditional phase-locked loops (PLL) [12]. Such a framework is susceptible to local minima and often presents additional block processing complexities which fail in low SNR conditions. Due to operation in low SNR environments, combined timing recovery and turbo decoding algorithms are unavoidable in future wireless cellular mobile systems.

The results in [13, 14] have shown that classical soft-input/soft-output (SISO) iterative detection/decoding algorithms embed timing parameter estimation in the decoding process. For instance in [14], combined iterative decoding, equalization and timing error estimation are performed with modified forward and backward recursions in the SISO decoders using a per-survivor processing algorithm [21]. Such methods are reliable but increase the receiver's design complexity with vast memory requirement. In order to reduce the complexity involved in designing the decoder structure, soft information provided at each iteration by a conventional turbo decoder can be used to derive reliable information on timing error estimation. This is the essence of the turbo principle synchronization technique [7] [22]. Though recent research focused the attention on turbo synchronization method [9, 10], achieving a fast converging timing recovery process has been under investigation,. timing phase vector representations for accurate lower bound variance estimation has been given less research attention. In order to improve on QoS provisioning in mobile networks, a bandwidth and power efficient based timing recovery method must be investigated.

The objective of this paper is to develop a soft timing recovery method for wireless mobile receivers. The proposed soft timing recovery method incorporates both bandwidth and power efficient communication systems for QoS applications in mobile networks. This goal is achieved by combining discrete polyphase matched

filtering, a soft iterative demapper and turbo decoder and a modified Newton-Raphson method. The derived timing phase estimator variance is investigated for the Cramer-Rao lower bound.

This paper is organized as follows. Section 1 provided a broad overview of the problem area, related work and results achieved by other researchers. In section 2, the base-band turbo system model is presented. In section 3, an improved soft timing recovery framework is proposed. Simulation tests and results are presented in sections 4 and 5. Conclusions are presented in section 6.

## 2. MOBILE COMMUNICATION SYSTEM MODEL

### 2.1 The Transmitter System Model

In section 2.1, the base band equivalent of a cellular transmitter model is shown in Figure 1. It consists of vocoder, turbo encoder, bit interleaved coded multilevel phase shift modulator and square root raised cosine filter. The vocoder generates 260 bits of compressed data every 20 ms at a bit rate of 13kbps. The generated bits are passed on to the turbo encoder in which redundancy bits are added to check and control channel errors. The considered turbo encoder comprises two recursive systematic convolutional encoders (RSC), which are separated with a pseudo-random -bits interleaver (INT) matrix denoted as  $\pi$ . The interleaver matrix can be assumed to be an identity matrix without loss of accuracy and also for computational simplicity reasons. Redundant bits are then appended to the wireless cellular mobile information bit sequence according to the information sequence's sensitivity to channels errors [2]. The encoder output is finally punctured to a net code rate of  $\frac{1}{2}$ , giving an overall bit rate of about 45.6kbps. This provides for an increase in the full bit rate of 22.8kbps standard with classical GSM/GPRS/EDGE coding techniques. The GSM/GPRS/EDGE is a time division multiplexing access (TDMA) system thus time bursts of 0.577ms duration are transmitted via radio channel. Several time bursts are usually specified in TDMA mobile networks. Examples include normal burst, a/an frequency correction burst, a/an synchronization burst, a/an access burst etc. For instance a normal time burst has 148 bits and is contained in one time slot. In principle, every time slot contains 156.25 bits' duration including 8.25 bits' duration for guard band reservation. This time slot is assigned a single user and can be multiplexed among eight different users through TDMA at a specific carrier frequency. The most important point to note here is that in TDMA normal burst, about 26 bit sequence is conveyed for receiver equalization and other

estimation functions such as timing recovery. However, there are bandwidth and power costs involved in such schemes. In order to mitigate bandwidth and power constraints and still transmit the same information, a multilevel phase shift modulation preceded by a nearly zero intersymbol interference pulse shaped filter must be considered. The multilevel phase shift keying mapper would give grouped symbols from the interleaved bit sequence in accordance with the expression [4] [12] and [15],

$$a_k^g = \sum_{q=1}^Q x_q \cdot 2^q \quad \forall q \in \{1, \dots, Q\}, \text{ and } \forall \mathbf{x} \in \mathbf{c} \quad (1)$$

where  $Q$  is the number of coded bits contained in a symbol,  $\mathbf{x}$  is the sequence of multilevel modulation

scheme consisting of  $Q$  bits each and  $\mathbf{c}$  is the sequence of coded bits. The grouping function in (1) is followed by the bit to symbol mapping represented as,

$$a_k = \mu(a_k^g) \quad (2)$$

where  $a_k$  and  $\mu, \mu$ , are respectively a  $k$ th complex symbol and a labelling mapping function.

The base band modulated (mapped) symbols are constrained into channel waveform filter for definite symbol rate. The time domain and frequency domain raised cosine filter characteristics are depicted in Figures 2a and 2b.

The raised cosine pulse shaping filter also provides zero

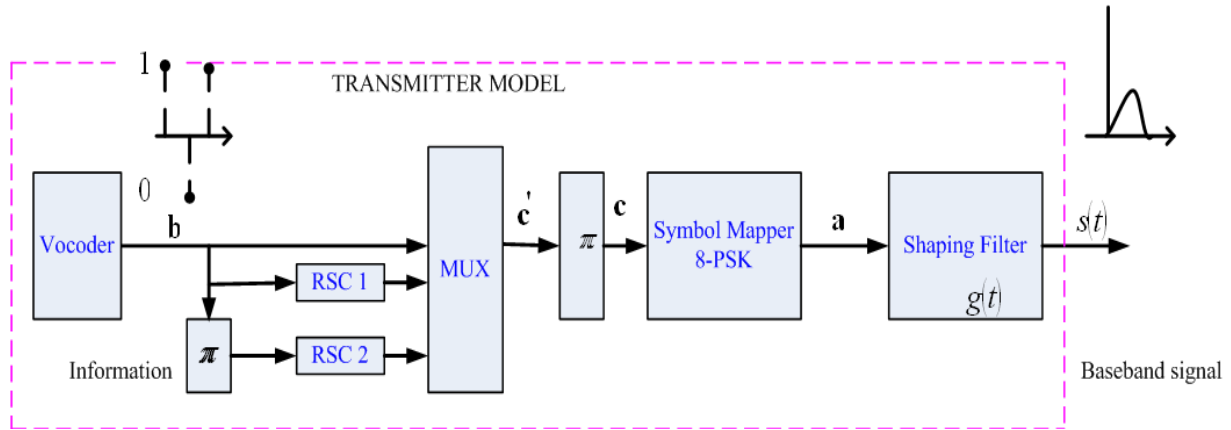


Figure 1: Transmitter base-band system model

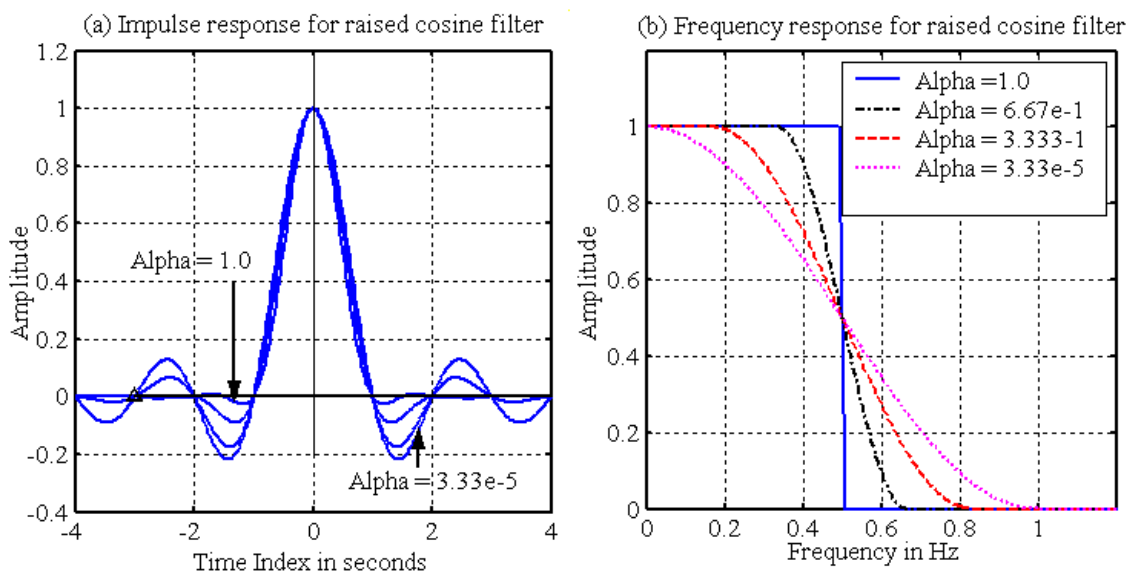


Figure 2: Raised cosine filter characteristics. a) Time domain. b) Frequency domain

intersymbol interference and an adjustable excess bandwidth known as roll-off parameter. The roll-off parameter allows for trade-off between bandwidth and time domain wave-shape.

Clearly, as the roll-off parameter alpha in Figure 2 varies from 0 to 1, there is more time-domain tail suppression at the cost of the increased bandwidth.

In a multipath radio channel, such as the case for GSM/GPRS/EDGE networks, severe intersymbol inference may be reduced by choosing about 35% excess bandwidth parameter. The pulse shaped transmit filter output is modelled in base band formalism as

$$s(t) = \sum_{k=-\infty}^{\infty} a_k g(t - kT) \quad (3)$$

where  $g(t)$  is the filter impulse response in time domain and  $T$  is the symbol period  $-\infty \leq k \leq \infty$ , observed over a large interval.

## 2.2 The Channel Model

Since the wireless terrestrial radio propagation of mobile traffic suffers from delays and attenuations caused by multipath fading, in section 2.2 the multipath fading is modelled by a linear time-variant filter characterized by the complex-valued low-pass equivalent channel impulse response (CIR) [18, 19],

$$h_c(t) = \sum_{n=1}^N \alpha_n(t) e^{j\phi_n(t)} \delta(t - \tau_n(t)). \quad (4)$$

Here,  $N$  is the number of propagation paths modelled as filter taps,  $\alpha_n(t)$  is the amplitude,  $\phi_n(t)$  is the phase, and  $\tau_n(t)$  is the timing phase shift, respectively of the mobile signal passing through an  $n$ th radio channel path.

If we hypothesize that in TDMA  $\tau_n(t)$  is separated from

$\tau_{(n+1)}(t)$  at symbol rate then the following statistical definitions can be assumed:

$$T_d \leq T \leq T_c, \quad (5)$$

where  $T_d$  is the delay spread which must satisfy

$$\sup_{n,n+1,t} [\tau_n(t) - \tau_{(n+1)}(t)] \leq T_d \quad (6)$$

and  $T_c$  is the coherence time.

This delay spread described by (6) measures in part the radio channel scattering effects hence a contribution to multipath fading. The multipath fading is modelled as Rayleigh distribution.

On the other hand  $T_c$  must satisfy

$$\sup_{s,n,t;|s-t|} f_c [\tau_n(t) - \tau_n(s)] \ll 1, \quad (7)$$

where  $f_c$  is the carrier frequency of the pass-band signal,

$\tau_n(t)$  and  $\tau_n(s)$  are the timing offsets of the  $n$ th path observed at different times,  $t$  and  $s$  respectively. The coherence time is thus, the period over which the pass-band cellular signal essentially remains time invariant. These statistical definitions presented in (5), (6) and (7) allow the continuously time varying signal to be assumed as an ergodic and piecewise-constant stochastic process. After the above analysis, the transmitted signal in (3) is convolved with the CIR in (4) and transmitted through an additive white Gaussian noise for atmospherically generated interferences.

## 2.3 The Receiver System Model

In section 2.3, the received signal vector  $\mathbf{r}$  assumes the form

$$r(t) = \sum_{n=1}^N \alpha_n(t) s(t - \tau_n(t)) e^{j\phi_n(t)} + n(t). \quad (8)$$

Here,  $n(t)$  is the time-variant additive white Gaussian noise with independent and identical distribution and variance is  $N_0 / 2$ .

$$r(t) = \sum_{n=1}^N \alpha_n(t) e^{j\phi_n(t)} \left\{ \sum_{k=0}^{K-1} [a_k g(t - kT - \tau_n(t))] \right\} + n(t) \quad (9)$$

The goal here is to estimate the timing offsets. The other nuisance unknown parameters can be grouped together as followings:

$$r(t) = \sum_{n=1}^N A_n(t) \left\{ \sum_{k=0}^{K-1} a_k g(t - kT - \tau_k(t)) \right\} + n(t) \quad (10)$$

where  $A_n(t) = \alpha_n(t)e^{j\phi_n(t)}$ , is treated as a nuisance parameter in the estimation of the timing delay. The notation  $\{\tau_k(t)\}$  is a set of time varying  $k$ th symbol timing offset parameter to be estimated over all multipath channels. In order to collect sufficient statistics for a decoding module, the received signal is first low pass filtered by anti-aliasing filter then sampled at a rate of  $1/T_s$ ,

where  $T_s < T/(1+\alpha)$  satisfying the Nyquist sampling theorem:

$f_s \geq 2/T$  where  $f_s = 1/T_s$ . When  $L$  samples are taken over each symbol, the total samples of the observation vector  $\mathbf{r}$  will be defined by

$$\begin{aligned} r_l &\equiv r(lT_s) \\ &= \sum_{k=0}^{LK-1} a_k g(lT_s - kT - \tau_k(lT_s)) + n(lT_s) \end{aligned} \quad (12)$$

#### 2.4 Discrete Matched filtering for fast timing recovery

In order to achieve the required timing resolution of  $M \times L$  samples per symbol from timing phase-corrected complex base band signal given in (12), an up sampling of  $r(lT_s)$  by a factor of  $M$  to obtain  $r(lT_s/M)$  must be performed in section 2.4. The resulting signal is filtered via a discrete matched root raised cosine filter whose output yields [21, 22],

$$y(lT_s/M) = \sum_{k=0}^{MLK-1} r((l-k)T_s/M) g(kT_s/M). \quad (13)$$

The matched filter output is down sampled to produce  $L$  samples per symbol where one of the samples is as close to  $y(lT_s + \tau_k)$  as the resolution allows. The polyphase decomposition of  $r(lT_s/M)$  yields only  $M$ th nonzero values of the FIR filter,

$$r(lT_s/M) = \begin{cases} r(lT_s), & l = 0, M, 2M, \dots \\ 0, & \text{otherwise} \end{cases} \quad (14)$$

At initial timing instant, these nonzero values in (14) coincide with the filter coefficients  $g(0)$ ,  $g(MT_s)$ ,

$g(2MT_s) \dots$  and the matched filter output may be expressed as

$$y(lT_s) = \sum_{i=0}^{LK-1} r((l-i)T_s) g(iT_s). \quad (15)$$

At the next timing instant, the nonzero values in (15) coincide with the filter coefficients  $g(1)$ ,  $g(MT_s + 1)$ ,

$g(2MT_s + 1)$ , and the matched filter output is expressed as

$$y((l-1/M)T_s) = \sum_{i=0}^{LK-1} r((l-i)T_s) g((i+1/M)T_s). \quad (16)$$

At the  $m$ th timing instant, the nonzero values in (16) coincide with the coefficients  $g(m)$ ,  $g(MT_s + m)$ ,  $g(2MT_s + m), \dots$

$$\begin{aligned} &y((l-m/M)T_s) \\ &= \sum_{i=0}^{LK-1} r((l-i)T_s) g((i+m/M)T_s). \end{aligned} \quad (17)$$

From the equations (15) through (17),  $M$  filter-banks have simultaneously input data samples  $r(lT_s)$  and the desired timing phase shift of the matched filter output is selected by connecting the matched filter output to appropriate filter in the filter-bank. However, the timing phase shift is unknown and soft decision iterative turbo receiver is employed to generate reliable estimates [6] [10]. In this sequel, the maximum likelihood estimation of the desired phase shift from SISO exchanges will be derived.

### 3. SOFT TIMING RECOVERY FOR MOBILE SYSTEMS

In this section we show how decoder functions can be improved with timing recovery with little modifications. We further introduce the concepts of a low variance design for a soft timing recovery in digital mobile receivers.

#### 3.1 Estimating timing information

The problem addressed in section 3.1 is the estimation of  $\boldsymbol{\tau} = [\tau_0, \tau_1, \dots, \tau_{K-1}]^T$  subject to a trial  $\tilde{\boldsymbol{\tau}} = [\tilde{\tau}_0, \tilde{\tau}_1, \dots, \tilde{\tau}_{K-1}]^T$ .

This estimate may be seen as the solution of the maximization problem

$$\hat{\boldsymbol{\tau}} = \underset{\boldsymbol{\tau}}{\operatorname{argmax}} \Lambda(\boldsymbol{\tau}) \quad (18)$$

Here,

$$\Lambda(\boldsymbol{\tau}) = \ln p(\mathbf{y} | \boldsymbol{\tau}) \quad (19)$$

and

$$p(\mathbf{y} | \boldsymbol{\tau}) = \int_{\mathbf{a}} p(\mathbf{a}) p(\mathbf{y} | \mathbf{a}, \boldsymbol{\tau}) d\mathbf{a}, \quad (20)$$

where,  $p(\mathbf{a})$  is a prior probability mass function. The logarithmic function of second factor of the integrand in (20) is defined as

$$\ln p(\mathbf{y} | \mathbf{a}, \boldsymbol{\tau}) = \Re \left\{ \sum_{k=0}^{N-1} a_k^* y(kT + \tilde{\tau}_k) \right\} \quad (21)$$

where  $y(kT + \tilde{\tau}_k)$  corresponds to a single stage matched filter output evaluated at  $kT + \tilde{\tau}_k$ . In order to solve for (18), we take the derivative of (19) with respect to  $\boldsymbol{\tau}$  and we equate to zero, namely

$$\begin{aligned} \frac{\partial}{\partial \boldsymbol{\tau}} \ln p(\mathbf{y} | \boldsymbol{\tau}) &= \\ &= \int_{\mathbf{a}} \frac{p(\mathbf{a}) p(\mathbf{y} | \mathbf{a}, \boldsymbol{\tau})}{p(\mathbf{y} | \boldsymbol{\tau})} \frac{\partial}{\partial \boldsymbol{\tau}} \ln p(\mathbf{y} | \mathbf{a}, \boldsymbol{\tau}) d\mathbf{a} = \mathbf{0}. \end{aligned} \quad (22)$$

We notice that the evaluation of (22) requires the knowledge of the priori probabilities,  $p(\mathbf{a})$  of the transmitted symbols at the receiver. However, in this problem, we assume that such information can only be derived from posteriori information. If we invoke Baye's rule in the first factor of the integrand in (22), we have a posteriori conditional probability density function (PDF) of the transmitted vector  $\mathbf{a}$ . We can then represent it as

$$\frac{p(\mathbf{a}) p(\mathbf{y} | \mathbf{a}, \boldsymbol{\tau})}{p(\mathbf{y} | \boldsymbol{\tau})} = p(\mathbf{a} | \mathbf{y}, \boldsymbol{\tau}). \quad (23)$$

Since vector  $\mathbf{r}$  from (8), is a function of vector  $\mathbf{n}$  but  $\mathbf{n}$  is not a function of  $\boldsymbol{\tau}$ , we can ignore  $\mathbf{n}$  in the following definition without loss of generality. We had indicated that the interleaving matrix is an identity matrix in section 2A, hence (23) becomes

$$p(\mathbf{y} | \mathbf{a}, \boldsymbol{\tau}) = f_{\mathbf{n}}(\mathbf{y} - \mathbf{H}(\boldsymbol{\tau})\mathbf{a}) = \exp\left(-\frac{\|\mathbf{y} - \mathbf{H}(\boldsymbol{\tau})\mathbf{a}\|^2}{N_0}\right) \quad (24)$$

The maximum likelihood estimation problem in (18) now becomes an expectation problem given as follows

$$\begin{aligned} \frac{\partial}{\partial \boldsymbol{\tau}} \ln p(\mathbf{y} | \boldsymbol{\tau}) &= \\ &= \int_{\mathbf{a}} p(\mathbf{a} | \mathbf{y}, \boldsymbol{\tau}) \frac{\partial}{\partial \boldsymbol{\tau}} \left\{ \Re \left\{ \sum_{k=0}^{N-1} a_k^* y(kT + \tilde{\tau}) \right\} \right\} \\ &= E_{\mathbf{a}} \left\{ \frac{\partial}{\partial \boldsymbol{\tau}} \ln p(\mathbf{y} | \mathbf{a}, \boldsymbol{\tau}) | \mathbf{y}, \boldsymbol{\tau} \right\} = \mathbf{0}. \end{aligned} \quad (25)$$

Since  $\boldsymbol{\tau}$  appears in both factors of the expectation problem in (25), the solution of (25) is non-trivial. According to [17], an iterative approach that generates a set of values for  $\hat{\boldsymbol{\tau}} = \{\hat{\tau}^1 \dots \hat{\tau}^i \dots \hat{\tau}^n\}$  is a possible solution. It is possible to prove that in the limit as  $n \rightarrow \infty$  the sequence of the timing estimate converges to a desired solution [19]. However, the proof is analytically complex. Fortunately, an iterative receiver employing turbo codes will help in achieving faster convergence [28].

Since a fast converging estimator is required for our problem, the modified Newton-Raphson method in [17] is applied to (25) to give a numerical solution presented in [32],

$$\hat{\boldsymbol{\tau}}^{(i)} = \hat{\boldsymbol{\tau}}^{(i-1)} \pm \left( \frac{\partial^2 \tilde{\Lambda}(\boldsymbol{\tau})}{\partial \boldsymbol{\tau}^2} \right)_{\boldsymbol{\tau}=\hat{\boldsymbol{\tau}}^{(i-1)}}^{-1} \left( \frac{\partial \tilde{\Lambda}(\boldsymbol{\tau})}{\partial \boldsymbol{\tau}} \right)_{\boldsymbol{\tau}=\hat{\boldsymbol{\tau}}^{(i-1)}} \quad (26)$$

$$\text{Here, } \mathbf{F} = \begin{bmatrix} \frac{\partial^2 \tilde{\Lambda}(\boldsymbol{\tau})}{\partial \tilde{\tau}_0^2} & \cdots & \frac{\partial^2 \tilde{\Lambda}(\boldsymbol{\tau})}{\partial \tilde{\tau}_0 \partial \tilde{\tau}_{K-1}} \\ \vdots & \ddots & \vdots \\ \frac{\partial^2 \tilde{\Lambda}(\boldsymbol{\tau})}{\partial \tilde{\tau}_{K-1} \partial \tilde{\tau}_0} & \cdots & \frac{\partial^2 \tilde{\Lambda}(\boldsymbol{\tau})}{\partial \tilde{\tau}_{K-1}^2} \end{bmatrix} \quad (27)$$

and

$$\begin{aligned} \mathbf{f}' &= \left[ \frac{\partial}{\partial \tilde{\tau}_0} \tilde{\Lambda}(\tilde{\tau}_0), \dots, \frac{\partial}{\partial \tilde{\tau}_{K-1}} \tilde{\Lambda}(\tilde{\tau}_{K-1}) \right]^T = \mathbf{0}. \\ &= \sum_{k=0}^{K-1} \left[ \Re \{ P(a_k) a_k^* \} \frac{\partial}{\partial \tilde{\tau}_k} y(kT + \tilde{\tau}_k) \right]_{\tilde{\tau}=\hat{\boldsymbol{\tau}}} = \mathbf{0}, \\ &= \sum_{k=0}^{K-1} \Re \{ \eta_k^* \dot{y}(kT + \hat{\tau}_k) \} = \mathbf{0}. \end{aligned} \quad (28)$$

The choice of sign  $\pm$  in (26) is described by the eigenvectors of  $\mathbf{F}$  for a non-singular matrix solution as discussed in [32].

The notation  $\eta_k^*$  in (28) defines a *a priori mean information* complex conjugate variable of the transmitted symbol  $a_k$ .

The a priori mean information is defined as

$$\eta_k^* = \sum_{a \in \mathbf{B}} a_k^* \left( x_k^1, x_k^2, \dots, x_k^Q \right) P \left( a_k \left( x_k^1, x_k^2, \dots, x_k^Q \right) \right) \quad (29)$$

where  $(x_k^1, x_k^2, \dots, x_k^Q)$  are the Q coded bits in a multilevel symbol modulation scheme [32]. According to [29], the soft information demapper computes posteriori probabilities from bit priori probabilities in low SNR environments. This is performed as follows,

$$P(x_k^1, x_k^2, \dots, x_k^Q) \approx P(x_k^1) P(x_k^2) \dots P(x_k^Q), \\ \triangleq \prod_q P(x_k^q) \quad (30)$$

The soft demapper also computes soft information defined by the log-likelihood ratio (LLR) on each a posteriori probability in order to achieve a wider dynamic range of decision levels as follows:

$$\lambda^{12}(x_k^q | \mathbf{y}; p) = \lambda^{12}(x_k^q | \mathbf{y}; e) + \lambda^{12}(x_k^q; i) \quad (31)$$

Here,

$$\lambda^{12}(x_k^q, \tilde{\tau}_k | \mathbf{y}; e) = \\ \log \frac{\sum_{\forall \mathbf{x}: x_k^q=0} p(\mathbf{y} | \tilde{\tau}, \mathbf{x} \in \mathbf{B}) \prod_{i=1: i \neq k}^{2N} P(x_{\forall k}^i)}{\sum_{\forall \mathbf{x}: x_k^q=1} p(\mathbf{y} | \tilde{\tau}, \mathbf{x} \in \mathbf{B}) \prod_{i=1: i \neq k}^{2N} P(x_{\forall k}^i)} \quad (32)$$

As shown in [8], the log-maximum a posteriori (Log-MAP) decoding algorithm of (32) becomes,

$$\lambda^{21}(b_k^q, \tilde{\tau}_k; p) = \\ \log \frac{P\{b_k^q = 0 | \lambda^{21}(\mathbf{c}; i), \lambda^{21}(\hat{\mathbf{b}}; i), decode\}}{P\{b_k^q = 1 | \lambda^{21}(\mathbf{c}; i), \lambda^{21}(\hat{\mathbf{b}}; i), decode\}} \forall k. \quad (33)$$

On the other hand, the Viterbi algorithm [30] computes the SISO from (32), as follows

$$\lambda^{21}(a_k, \tilde{\tau}_k; p) = \frac{1}{\alpha} \log \frac{1 + e^{(\alpha \lambda^{21}(a_k; i) + \Delta)}}{e^{(\Delta)} + e^{(\alpha \lambda^{21}(a_k; i))}}, \quad (34)$$

where  $\alpha = 4d_{free} E_s / N_0$  and  $\Delta$  are the two path metric differences in the trellis structure presented in [30].

The a posteriori mean can now be computed from the soft information,

$$\eta_k = \sum_{\vartheta_m \in \mathbf{B}} \vartheta_m P(a_k = \vartheta_m | \mathbf{y}, \tilde{\tau}_k), \quad (35)$$

where

$$P(a_k = \vartheta_m, \tilde{\tau}_k | y_k) = \frac{\exp(-\vartheta_m \lambda^{21}(a_k = \vartheta_m, \tilde{\tau}_k | y_k))}{1 + \exp(-\lambda^{21}(a_k = \vartheta_m, \tilde{\tau}_k | y_k))}. \quad (36)$$

The a priori mean information in (29) is now approximated as a posteriori mean information in (35). Equations 33 and 34 present the log-MAP and the soft output Viterbi algorithm (SOVA) based timing recovery methods, respectively. The log-MAP and SOVA based timing recovery equations are substituted in (35) for soft mean information. The soft mean information generates the soft timing phase signals as depicted in (26). This is achieved several iterations by the soft demapper-decoder system. The reliable soft timing phase signals are attained after the system has converged. Soft timing phases estimated in (26) update the discrete polyphase matched filter.

### 3.2 Updating timing phase estimates

In section 3.2, we begin the iteration by assuming that the previous,  $(i-1)$ th timing offset estimate is zero. The estimated timing offset finally updates the early and late samples of the discrete polyphase matched filter outputs and an optimal synchronization is attained when the early and late samples become equal [22, 25]. The new timing estimate will be based on the discrete polyphase matched filter output  $y(s)|_{s=kT+\tilde{\tau}^{i-1}}$  as shown in Figure 3 and the mean of posterior probabilities  $\eta_k^{(i-1)}$  from the previous iteration. This phenomenon can be seen in

$$\left( \frac{\partial \tilde{\Lambda}(\tilde{\tau})}{\partial \tilde{\tau}} \right)_{\tilde{\tau}=\tau^{(i-1)}} \approx \frac{\tilde{\Lambda}(\hat{\tau}^{(i-1)} + \Delta \hat{\tau}) - \tilde{\Lambda}(\hat{\tau}^{(i-1)} - \Delta \hat{\tau})}{2\Delta \hat{\tau}} \quad (37)$$

In low SNR and assuming a single filter stage case as given in [33], the expression in (37) is well approximated by

$$= 1/\Delta \hat{\tau} \sum_k \Re \left\{ \eta_k^{*(i-1)} \begin{pmatrix} y(kT + \hat{\tau}^{(i-1)} + \Delta \hat{\tau}) \\ -y(kT + \hat{\tau}^{(i-1)} - \Delta \hat{\tau}) \end{pmatrix} \right\} \quad (38)$$

and it easy to show that the second derivative in (37) is

$$= 1/\Delta \hat{\tau}^2 \sum_k \Re \left\{ \eta_k^{*(i-1)} \begin{pmatrix} y(kT + \hat{\tau}^{(i-1)} + \Delta \hat{\tau}) \\ +y(kT + \hat{\tau}^{(i-1)} - \Delta \hat{\tau}) \\ -2y(kT + \hat{\tau}^{(i-1)}) \end{pmatrix} \right\} \quad (39)$$

where  $\Delta \hat{\tau}$  is an adjustable advance/delay parameter that satisfies  $0 < \Delta \hat{\tau} < T/2$ .

### 3.3 Lower Bound on timing error variance

In many cases, the statistics of the observation depend not only on the vector parameter to be estimated, but also on a nuisance vector parameter we do not want to estimate [28]. In order to assess the variance performance of unknown parameter to be estimated, a Cramer-Rao bound (CRB) on an error variance of any unbiased estimate is normally derived [23, 26, 27]. The CRB based synchronizer has been applied in linearly modulated signals [28]. However, timing recovery in multilevel GSM modulation schemes with unknown data symbols as nuisance parameters is still a challenging task. This task is addressed in this subsection.

Our goal is to derive a lower bound on timing estimation error variance given a time-varying timing offset. We firstly model the timing offset as a random walk as in [33],

$$\begin{aligned} \tau_{k+1} &= \tau_k + \omega_{k+1} = \tau_{-1} + \sum_{j=0}^{k+1} \omega_j \\ &= \tau_k + (k+1)\Delta T. \end{aligned} \quad (40)$$

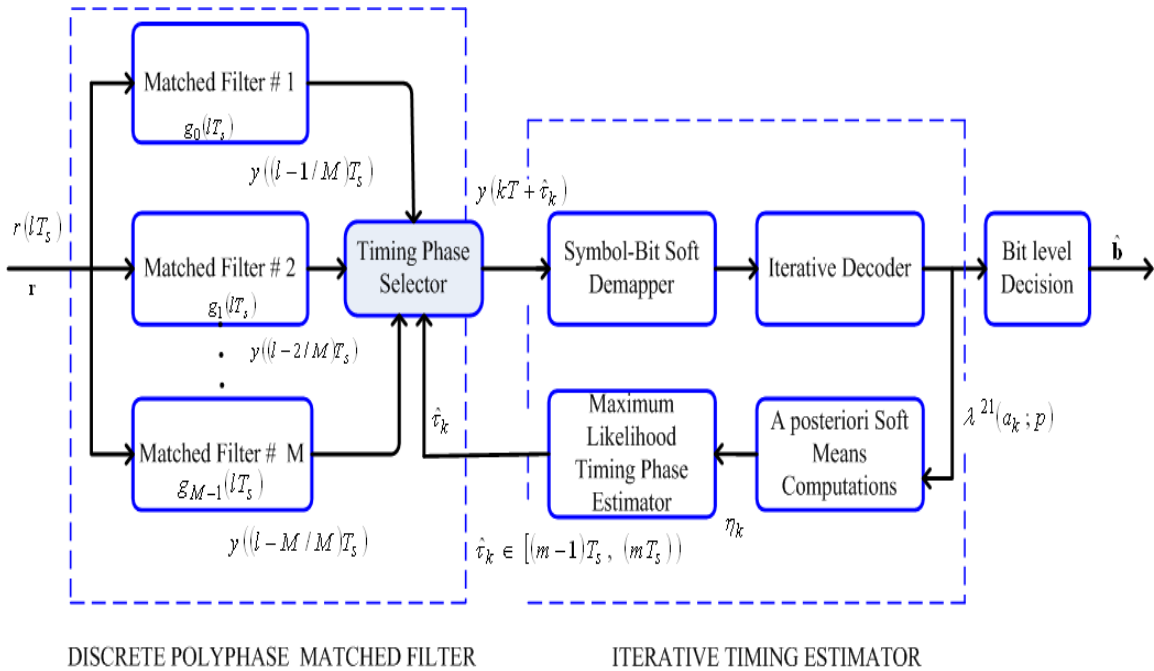


Figure 3: The iterative receiver structure

Here,  $\omega_k \in \mathcal{N}(\mathbf{0}, \sigma_\omega^2)$  are i. i. d. of  $k$ th symbol and  $\sigma_\omega^2$  determines the severity of the timing jitter. The random walk is chosen because of its simplicity and because of its ability to model a wide range of mobile channels. We assume a perfect acquisition by setting  $\tau_{-1} = \mathbf{0}$ . In [18], the CRB on the timing estimation error variance for a generic channel was presented. It was shown that the CRB is a lower bound on the estimation error variance of unbiased estimators of deterministic parameters  $\boldsymbol{\tau} = [\Delta T, \boldsymbol{\tau}]^T$ . In [19], the CRB is given by

$$\mathbb{E}_r \left[ (\hat{\tau}_i - \tau_i)^2 \right] \geq CRB_i(\boldsymbol{\tau}), \quad (41)$$

where  $CRB_i(\boldsymbol{\tau})$  is the  $i$ th diagonal element of the inverse of the Fisher information matrix  $\mathbf{J}(\boldsymbol{\tau})$ . The  $(i, j)$ th element of  $\mathbf{J}(\boldsymbol{\tau})$  is given by

$$\mathbf{J}(\boldsymbol{\tau}) = \mathbb{E}_r \left[ -\frac{\partial^2}{\partial \tau_i \partial \tau_j} \ln(p(\mathbf{r} | \boldsymbol{\tau})) \right]. \quad (42)$$

The probability density  $p(\mathbf{r} | \boldsymbol{\tau})$  of  $\mathbf{r}$ , corresponding to a given value of  $\boldsymbol{\tau}$ , is called the likelihood function of  $\boldsymbol{\tau}$ .

The expectation  $\mathbb{E}_r[\cdot]$  is with respect to  $p(\mathbf{r} | \boldsymbol{\tau})$ . Equivalently (42) can be re-written as

$$\mathbf{J}(\boldsymbol{\tau}) = \mathbb{E} \left\{ \left[ \frac{\partial}{\partial \boldsymbol{\tau}} \ln p(\mathbf{r} | \boldsymbol{\tau}) \right] \left[ \frac{\partial}{\partial \boldsymbol{\tau}} \ln p(\mathbf{r} | \boldsymbol{\tau}) \right]^T \right\} \quad (43)$$

From a detailed proof in [20], we obtain Cramer-Rao bound as

$$\frac{\mathbb{E} \left[ (\tau - \hat{\tau})^2 \right]}{T^2} \geq \frac{2\sigma^2(2N-1)}{\left( \frac{2\pi^2}{3} - 1 \right) N(N+1)}.$$

$$\frac{\mathbb{E} \left[ (\Delta T - \hat{\Delta T})^2 \right]}{T^2} \geq \frac{2\sigma^2}{\left( \frac{2\pi^2}{3} - 1 \right) (N-1)N(N+1)} \quad (44)$$

where  $\sigma$  is the standard deviation of noise and other parameters retaining their definitions as we have given earlier.

#### 4. SIMULATION TESTS

To verify the performance of our turbo aided timing recovery scheme, we simulated a base band communication system transmitting an 8-constellation alphabet for phase shift keying (8-PSK) symbols in MATLAB. We considered a convolutional turbo code generator polynomial (23, 33) with punctured net rate of a  $\frac{1}{2}$ . The interleaver length was set to block sizes of 456 bits and a square root raised cosine signalling pulse with roll-off of 0.35 and 31 filter taps was used. 1000 blocks were transmitted over a Rician distributed flat fading channel with additive white Gaussian noise (AWGN). The received signal was passed through an anti-aliasing filter and then sampled at an incommensurate rate but higher than the baud rate or the symbol rate. A polyphase matched filtering structure was embedded at the input of the soft demapper and the turbo decoder to help with fast iterative soft timing phase estimation. In order to investigate for bit error rate (BER) and radio block error rate (BLER) performance, a Monte Carlo simulation methodology [31] was performed for GSM communication networks.

#### 5. RESULTS

In Figure 4, the transmitted symbol is compared to the output of the received discrete matched filter output. Early, late and on time samples per filter stage are taken from the discrete polyphase matched filter bank.

As the symbol sequences enter the filter stages with the timing phase shifts, the filter output samples are adjusted based on the soft timing information from the iterative receiver. For instance, in Figure 4 the received signal is shifted to the right with a length of samples equal to the soft timing phase generated from the estimator system. Further samples per symbol are taken in the next turbo iteration to compute new timing phase estimates. The new timing phase estimates adjust the received symbol sequence and the process repeats for the entire received symbol sequence.

Results in Figure 5 reveal a typical radio channel BER performance for wireless mobile networks. For simplicity in radio channel modelling, multipath flat fading is described by a Rician  $K$ -factor denoted by  $K = \beta^2 / 2\sigma_0^2$ . Here,  $\beta$  and  $\sigma_0^2$  are the amplitude of

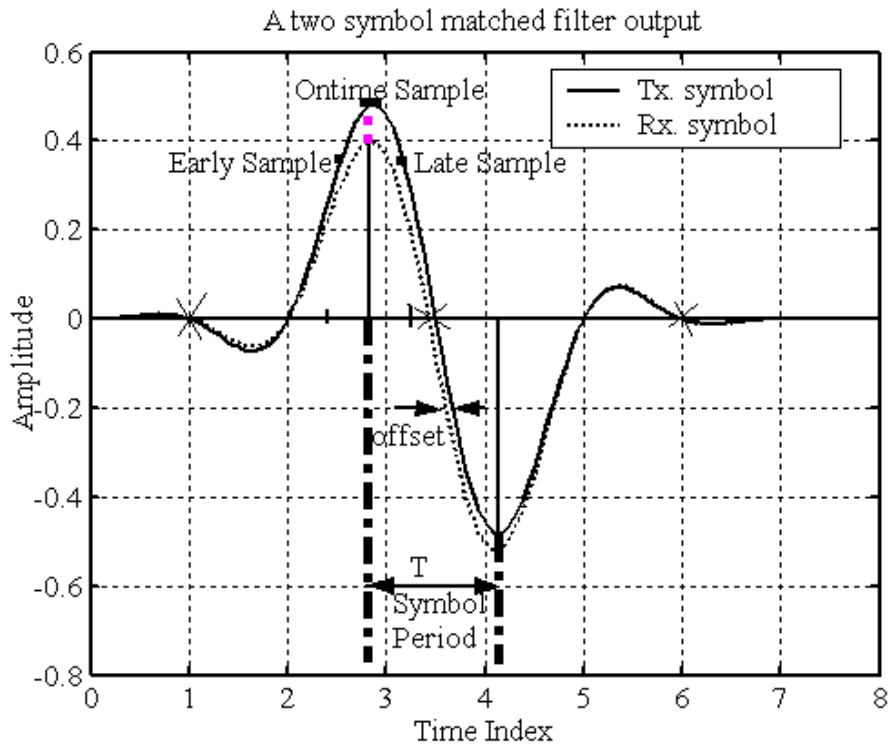


Figure 4: Matched filter signal for timing recovery scheme

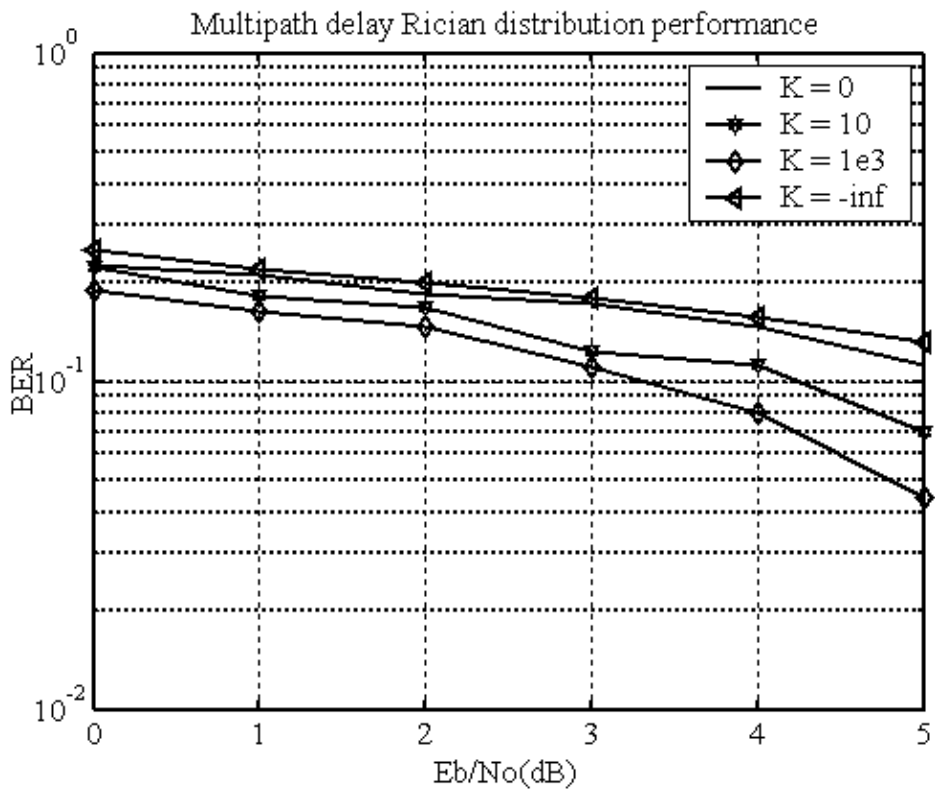


Figure 5: Wireless cellular radio channel performance

the specular path component (dominant line of sight) and variance of Gaussian random channel samples with zero-means, respectively. For instance a zero value of  $K$  means that there is no line of sight (LOS) between the transmitter and the receiver. In such scenarios, a Rician channel distribution is best modelled by a Rayleigh channel distribution. The Rayleigh channel distribution reveals severe channel conditions. The BER performance of synchronizers in Figure 5 is the worst when equal to negative infinity. It is necessary that wireless mobile receivers operating at a low signal to noise ratio i.e. at a low, require turbo codes to generate reliable soft timing estimates after many turbo iterations. This ensures a guaranteed QoS provisioning to end users at the expense of latency. In voice based receivers, latency is highly undesirable. Thus the generation of soft timing estimates is a trade off between number of turbo iterations and perfect synchronization.

The bit error rate (BER) performance of an iterative soft timing recovery based on the logarithmic maximum

likelihood a posteriori (Log-MAP) information is depicted in Figure 6. The soft information based on a combined maximum likelihood and iterative turbo timing recovery method outperforms conventional methods. The results in Figure 6 reveal desirable BER performances: steady waterfall and minimum error floor region within a short span of a SNR at low measurements, i.e. 1-2.5dB. The proposed method yields low BER compared to a data-aided Viterbi detection based synchronizer and a classical early-late synchronizer. This is explained by the fact that in low SNR scenarios, data aided and early-late gate methods assume that neighbouring symbols of the received signal are statistically independent and thus the received signal is deterministic a priori. However, the assumption fails in severe channel distortions. The receiver must therefore resort to blind timing recovery methods. In the proposed method, the unknown a priori bit probabilities are approximated by posteriori computations.

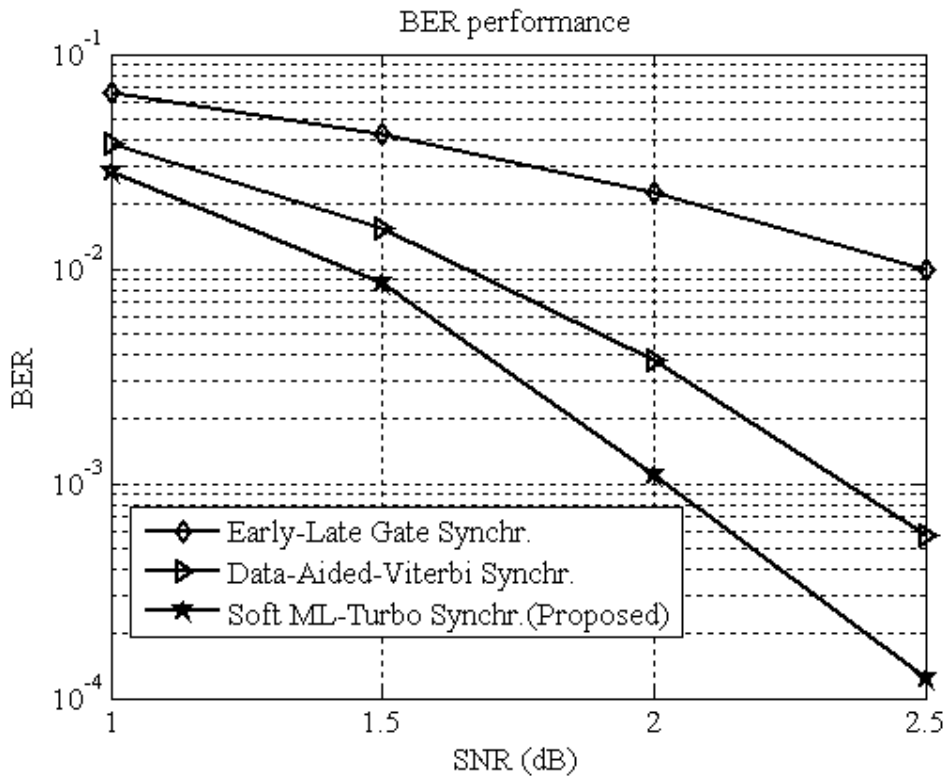


Figure 6: Log-MAP based soft timing recovery method for BER

In Figure 7 the block error rate (BLER) performance of an iterative soft timing recovery based on the Log-MAP information is shown. The proposed method outperforms conventional methods. In the log-MAP based timing recovery scheme, the BER and BLER perform well at low SNR, which is highly desirable for wireless cellular mobile systems. In recent publications data-aided synchronizers are known to be more reliable than the classical decision-directed synchronizers, but the BER and BLER performance indicated by Figures 6 and 7 respectively, show that the proposed timing recovery scheme yields a better performance. This is because of stochastic channel conditions and low SNR environments that make it difficult for the receiver to extract correct clock signals from the received sequence. Unlike classical decision-directed timing recovery methods that give decisions from the limited dynamic probability range i.e. probability value

range from 0 to 1, the proposed method has a larger dynamic range for making decisions i.e. soft information are represented with probability ratios. Probability ratios range from 0 to infinity.

The results in Figure 8 show the soft output Viterbi algorithm (SOVA) BER performance compared to conventional methods. Like in log-MAP based synchronizers, the BER performance indicates desirable start-up, waterfall and error regions. The results indicate that the proposed method outperforms the conventional methods and the explanations motivating this observation are similar to the discussions for Figure 6. However, the data-aided timing recovery method performed closer to the proposed SOVA method. This can be explained by the fact that SOVA based turbo structures yield soft timing signals from signal sequences similar to simple Viterbi

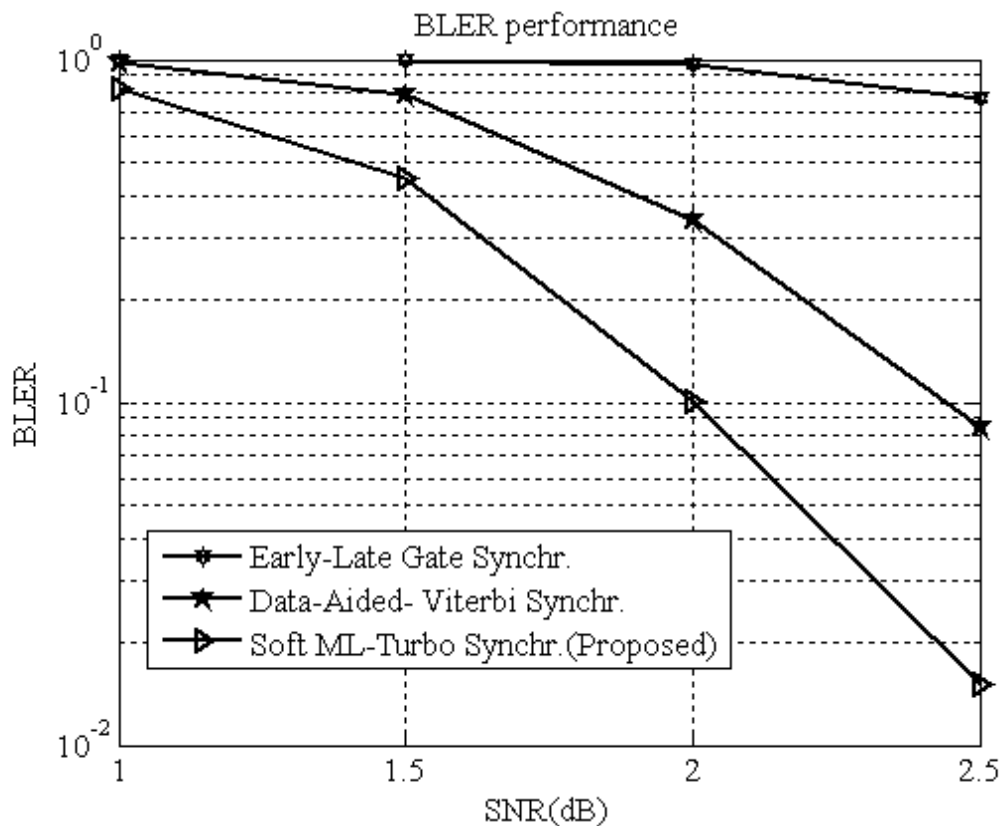


Figure 7: Log-MAP based soft timing recovery method for BLER

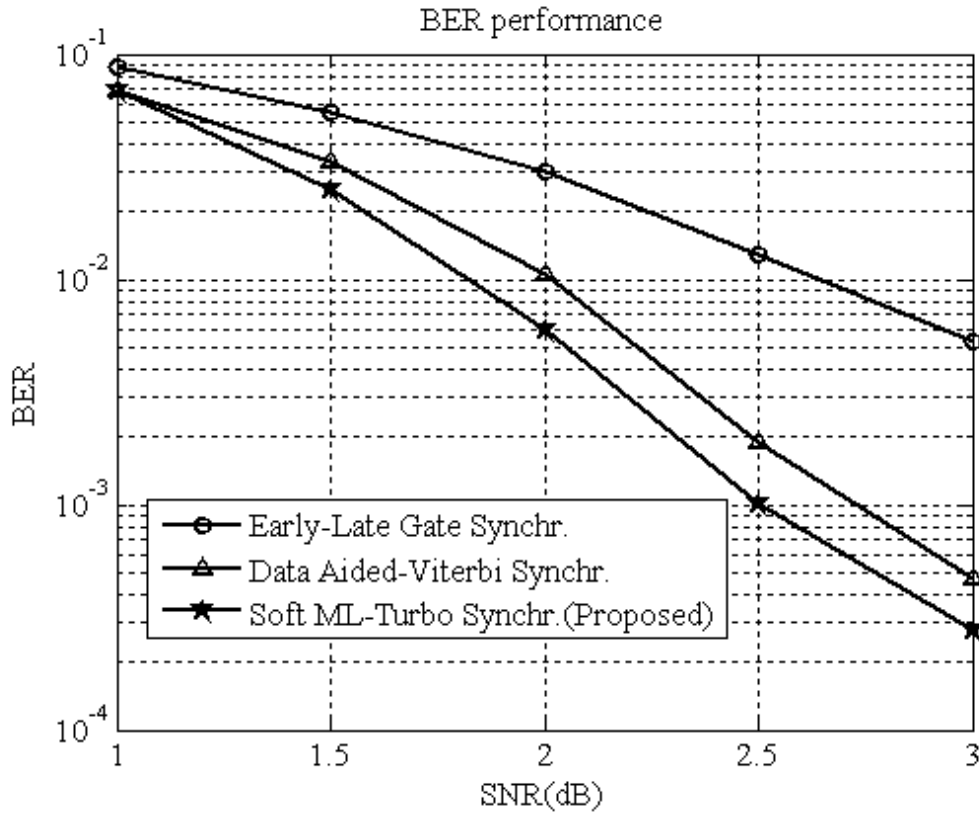


Figure 8: SOVA based soft timing recovery method for BER

based detectors. However, due to turbo codes, the proposed timing recovery in SOVA performs well in low SNR channels compared to the classical forward error correction codes in conventional methods.

The SOVA based timing recovery BLER performance compared to conventional methods are depicted in Figure 9. The proposed method provides lower BLER performance than conventional methods. The early-gate gate timing recovery yields the worst BLER performance in low SNR. This is due to the fact that the associated matched filter aiding the early-late gate timing recovery schemes is sub-optimal when neighbouring symbols are statistically dependent in noisy channels. In general, the BER and BLER of the proposed timing recovery method indicate good error floor, waterfall and start-up regions as expected. However, overall simulation results indicate that SOVA based timing recovery methods yield a degraded BER and BLER performance in low SNR compared to the log-MAP methods. The reason behind this can be explained by the fact that log-MAP timing recovery methods are computed

at individual bit level decision with high and required resolution to correct channel errors while the SOVA based timing recovery method operates at symbol level with low decision resolution. Moreover, bit sequences were interleaved at the transmitter end before being mapped in a spectrally efficient digital modulator. This bit level interleaving corrects error bursts more effectively than performing the interleaving at symbol level. Since turbo receivers employ a bit by bit demapper and de-interleaver, the presence of channel error bursts can easily be corrected. This leads to low BER and BLER performance and consequently improved QoS provisioning to the terminal mobile users. However, log-MAP based soft timing recovery methods yield more reliable soft timing signals at the expense of receiver's computational and structural complexities. The complexities constrain the mobile system's memory and battery power requirements. Such requirements are undesirable for mobile system operators. Thus, SOVA based soft timing recovery methods become an alternative method to provide QoS demands by both mobile operators and end users. However due to the

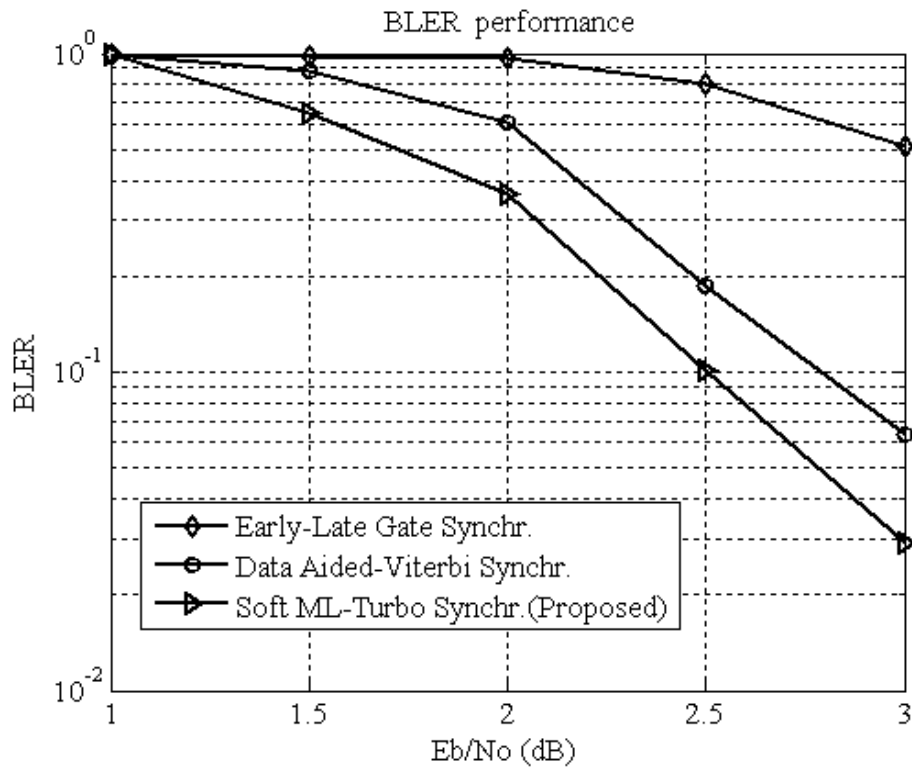


Figure 9: SOVA based soft timing recovery method for BLER

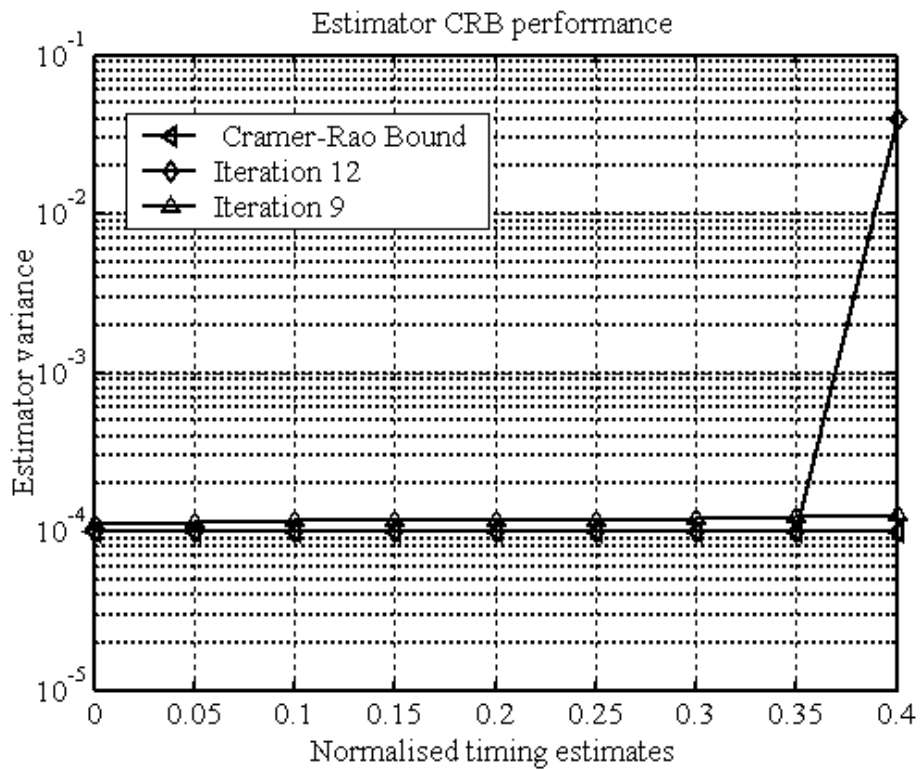


Figure 10: Estimator variance performance bound

presence of multiple nuisance parameters characterising the log-MAP and SOVA based soft timing estimators, the timing error variance must be investigated. The approach investigated is the theoretic Cramer-Rao bound (CRB).

In order to verify the Cramer-Rao bound on variance performance, the results in Figure 10 were obtained. It is evident that the proposed timing recovery method operates at low SNR at a tight lower theoretical bound i.e. CRB. In Figure 10 it is noted that by increasing the number of iterations, the variance performance improves to a desirable low value. However, for large normalized timing offsets i.e. 0.35, the system estimator becomes biased. This is regardless of any increase in the number of iterations. This biasness is the condition of timing phase ambiguity known in blind timing recovery estimators. It can be exploited as an advantage for cellular wireless mobile systems which trades off latency for reliability.

## 6. CONCLUSION

In conclusion, combined synchronization and decoding of turbo codes give good results in low SNR environments. In such applications timing recovery is extremely difficult with traditional methods. Deriving a good timing estimator function is crucial in both the decoding process and steady-state sampling phase. Deep channel fading and multipath effects degrade classical timing recovery methods, but an iterative soft timing recovery method improves the BER performance in such conditions. The mobile service operator requires a less memory-demanding and computationally intensive system in order to charge less but still need to make business profits while the terminal user requires a low cost and much reliable receiver system. However, satisfying all these conditions in low SNR would imply trading off QoS improvement in wireless mobile applications. Fortunately, reduced complex soft timing recovery methods are now possible with the proposed SOVA based soft timing recovery methods. The overall BER and BLER performances in the above simulation tests reveal a decrease in BER and BLER with increase in signal to noise ratio. This is because iterative soft timing phase estimations generate reliable timing signals which update the discrete polyphase matched filter stages. The outputs of the filter stages improve the demapping and decoding time and leads to faster convergence. The iterative receiver system's fast convergence suits its application to mobile networks where delay variations are undesirable. However, the reliability of soft timing phase estimates improves with an increasing number of turbo iterations. This may cause

latency and a choice on the maximum number of turbo iterations for good QoS provisioning becomes necessary. In order to investigate how to choose the optimum number of turbo iterations, results in Figure 10 indicate that for a large timing offset estimation, say 0.35 the timing phase estimator becomes biased. The biased variance performance at many iterations for ambiguous timing phases, aide in the choice of optimum number of iterations for QoS provisioning. Hence, the proposed soft timing phase estimation is a viable solution for mobile receiver applications. However, the proposed scheme is less complex than a scheme based on of training pilot sequences employed in wireless cellular mobile networks. The complexity involved can be traded-off for both power and bandwidth efficiencies in cellular applications. In future, more research should be conducted to mitigate turbo complexities to suit its application in 3<sup>rd</sup> generation mobile networks.

## ACKNOWLEDGEMENT

The author would like to acknowledge F'SATIE, the NRF, Telkom CoE and Tshwane University of Technology for their support.

## REFERENCES

- [1] A. Shanmugam and A. R. Abdul Rajak, "Optimal design of forward error correcting codes for wireless communication", [www.academicjournal.com](http://www.academicjournal.com), vol. 14, 2005.
- [2] CISCO, "Cisco mobile exchange solution guide: Overview of GSM, GPRS, and UMTS", [www.cisco.com](http://www.cisco.com), 2002.
- [3] C. E. Shannon, "A mathematical theory of communication", *Bell system technology journal*, vol. 48, pp. 379-423, 1948.
- [4] W. C. Lee, *Mobile communications engineering*. New York: Mc-Graw-Hill, 1982.
- [5] C. Berrou, A. Glavieux and P. Thitimajshima, "Near Shannon limit error-correcting coding and decoding: turbo codes," in *Proc. ICC 1993*, 1993, pp. 1064-1070.
- [6] C. Berrou and A. Glavieux, "Near optimum error correcting coding and decoding: turbo codes," *IEEE Trans. Commun.*, vol. 44, no. 10, pp. 1261-1271, 1996
- [7] J. Hagenauer, "The turbo principle: tutorial introduction and state of art," in *Proc. Int. Symposium on Turbo Codes and Related Topics*, pp. 1-11, Brest, France, September 1997.

- [8] M. Sellathurai and S. Haykin, "Turbo-Blast for wireless communications: theory and experiments," *IEEE Trans. Sig. Proc.*, vol. 50, no. 10, pp. 2538-2546, 2002
- [9] C. Herzet, V. Ramon, L. Vandendorpe, "Iterative soft-decision directed timing estimation for turbo receivers," *IEEE 9<sup>th</sup> Symposium on Commun., and Vehicular Technology*, pp. 97-101, 2003
- [10] N. Noels, V. Lottici, A. Dejonghe, H. Steendam, M. Moeneclaey, M. Luise, L. Vandendorpe, "A theoretical framework for soft-information-based synchronization in iterative(turbo) receivers," *EURASIP J. Wireless Commun., and Network.*, vol. 2, pp. 177-129, 2005.
- [11] K. H. Mueller and M. Muller, "Timing recovery in digital synchronous data receivers," *IEEE Trans. Commun.*, vol. Com-24, pp. 516-532, 1976.
- [12] J. G. Proakis and M. Salehi, *Communication systems engineering*. New Jersey: Prentice Hall, 2002.
- [13] J. R. Barry, A. Kavcic, S. W. McLaughlin, A. Nayak, and W. Zeng, "Iterative timing recovery," *IEEE Signal Processing Mag.*, vol. 2, pp. 89-102, 2004.
- [14] P. Kovintavewat, J. R. Barry, M. F. Erden, and E. M. Kurtas, "Robustness of per-survivor iterative timing recovery in perpendicular recording channels," *IEEE Trans. Magnetics*, vol. 10, pp. 807-808, 2005.
- [15] B. Mielczarek, *Turbo codes and channel estimation in wireless systems*, PhD Thesis, Signals and Systems, Chalmers University of Technology, Goteborg, 2002.
- [16] J. M. Walsh, C. R. Johnson, and P. A. Regalia, "Joint synchronization and decoding exploiting the turbo principle," in *Proc. Conf. Inform. Sciences and Systems*, 2004
- [17] D. Tabak and B. C. Kuo, *Optimal control by mathematical programming*. New Jersey: Prentice Hall, 1971.
- [18] H. Meyr, M. Moeneclaey, and S. Fechtel, *Digital communication receivers: Synchronization, channel estimation, and signal processing*. New York: John Wiley and sons, 1998.
- [19] H. L. Van Trees, *Detection, Estimation and Modulation Theory*. New York: John Wiley and sons, 1968.
- [20] A. Nayak, J. Barry and S. McLaughlin, "Joint Timing Recovery and Turbo Equalization for Coded Partial Response Channels," *IEEE Trans. Magnetics*, vol. 38, no.5, pp. 2295-2297, Sept 2002.
- [21] F. J. Harris and M. Rice, "Multirate digital filters for symbol timing synchronization in software defined radios," *IEEE journal on selected areas in commun.*, vol. 19, no. 12, pp. 2346-2357, 2001.
- [22] F. J. Harris, *Multirate signal processing for communication systems*. New Jersey: Prentice Hall, 2004.
- [23] C. L. Philips and H. T. Nagle, *Digital control system analysis and design*, 3<sup>rd</sup> ed. New Jersey: Prentice Hall, 1998.
- [24] A. Polydoros and K. M. Chugg, "Per Survivor processing (PSP)", [www.phys.uoa.gr/el-lab/polydoros/psp/psp.html](http://www.phys.uoa.gr/el-lab/polydoros/psp/psp.html), [Accessed on: 18/11/2005].
- [25] N. Noels, C. Herzet, A. Dejonghe, *et al.*, "Turbo synchronization: an EM interpretation," In Proc. IEEE international Conference on Communications (ICC '03), Anchorage, Alaska, USA, May 2003.
- [26] H. Cramer, *Mathematical Methods of Statistics*. Princeton, NJ: Princeton Univ. Press, 1946.
- [27] C. R. Rao, "Information and accuracy attainable in the estimation of statistical parameters," *Bull. Calcutta Math. Soc.*, vol. 37, pp. 81-91, 1945.
- [28] N. Noels, H. Wymeersch, H. Steendam and M. Moeneclaey, "The true Cramer-Rao bound for timing recovery from a bandlimited linearly modulated waveform with unknown carrier phase and frequency," *IEEE Transactions on Communications journal*, vol. 52, no. 3, pp. 473-483, March 2004.
- [29] R. Koetter, A.C. Singer and M. Tuchler, "Turbo equalization," *IEEE Signal Processing Magazine*, vol. 21, no. 1, pp. 67-80, January 2004.
- [30] J. Hagenauer and P. Hoher, "A Viterbi algorithm with soft-decision outputs and its applications," *IEEE Trans. Communication Journal*, vol. 47, pp. 1680-1686, 1989.
- [31] N. Metropolis and S. Ulam, "The Monte Carlo method," *American Statistic Association Journal*, vol. 44, pp. 335-341, 1949.
- [32] T. O. Olwal, M. A. van Wyk, D. Chatelain, M. Odhiambo and B. J. van Wyk, "Low variance timing recovery in turbo receivers," In Proc. *IEEE 13<sup>th</sup> International Conference on Telecommunication (ICT '06)*, Funchal, Portugal, May 2006.
- [33] T. O. Olwal, M. A. van Wyk, D. Chatelain, M. Odhiambo and B.J. van Wyk, "Cramer-Rao bound on timing recovery for GSM receivers," In Proc. *IEEE ICTe*